Article ID: 1000-324X(2023)02-0213-06 **DOI:** 10.15541/jim20220155

Zirconia Spacer: Preparation by Low Temperature Spray-coating and Application in Triple-layer Perovskite Solar Cells

ZHANG Wanwen[1], LUO Jianqiang[1], LIU Shujuan[1], MA Jianguo[1], ZHANG Xiaoping[1], YANG Songwang[2]

(1. Jiangxi Province Key Laboratory of Synthetic Chemistry, East China University of Technology, Nanchang 330013, China; 2. CAS Key Laboratory of Materials for Energy Conversion, Shanghai Institute of Ceramics, Chinese Academy of Sciences, Shanghai 201899, China)

Abstract: Perovskite solar cells (PSCs) with structure of TiO_2/ZrO_2/carbon triple-layer are attractive recently because of their inexpensive raw materials, scalable fabrication process, and outstanding stability. But little progress has been made in the low temperature fabrication of TiO_2/ZrO_2/carbon triple-layer structured PSCs. A major reason is that it is rather difficult to construct the ZrO_2 spacer layer at low temperature. Herein, we report a facile low-temperature spray-coating method to prepare effective ZrO_2 spacer layer in TiO_2/ZrO_2/carbon triple-layer PSCs using urea to tune the porosity. After optimizing the amount of urea and the thickness of zirconia to 1100 nm, power conversion efficiencies (PCE) of 14.7% for a single cell and 10.8% for a module with 5 cells connected in series (5×0.9 cm× 2.5 cm) were achieved. Furthermore, the PSCs could be stable for 200 d at constant temperature (25 ℃) and humidity (40%). With this spray coating method, the zirconia layer on flexible substrate can endure 50 times of bending without any cracking. Compared to the conventional screen-printing method of ZrO_2 spacer layer, the spray-coating alternative developed in this work shows advantages of more convenient to process, preparation under lower temperature, and compatibility to flexible substrate.

Key words: perovskite solar cell; triple-layer structure; low-temperature; zirconia; spray-coating

Perovskite solar cells (PSCs), firstly reported by Miyasaka, *et al*.[1] in 2009, has drawn tremendous attentions[2-5]. After years of intensive studies, PSCs showed great improvements on both power conversion efficiency (PCE) and stability[6-9]. PSCs are generally composed of the electron transporting layer, the perovskite light-absorbing layer, the hole transporting layer and two contact electrodes. Several architectures of PSCs were developed, such as fully-printable triple-layer PSCs, planar and inverted structured PSCs[10-14]. Among them, the fully-printable TiO_2/ZrO_2/carbon triple-layer PSCs own advantages of inexpensive raw materials, scalable fabrication process, and outstanding stability[15-17]. However, TiO_2/ZrO_2/carbon triple-layer PSCs requires delicate steps to fabricate screen printable pastes of TiO_2, ZrO_2 and carbon, including addition of organic additives, adjustment of viscosity, homogenization, *etc*. The pastes were then screen printed sequentially on substrate, and high temperature calcination is necessary to remove the organics. The high temperature process is incompatible with plastic flexible substrate, limiting the potential application of the TiO_2/ZrO_2 /carbon triple-layer PSCs.

In the PSCs research community, flexible substrate-compatible fabrication process is appealing[18-19]. In this context, a number of techniques were developed for building flexible planar or inverted structured PSCs, including sputtering, evaporation, low-temperature sintering[20-24]. But none of these methods are applicable to fabricate the TiO_2/ZrO_2/carbon triple-layer flexible PSCs. Chemical sintering of mesoporous titania layer at low-temperature were widely reported in dye-sensitized solar cells[25]. Recently, a low temperature method was developed to fabricate the carbon layer[26]. However, it is still challenging to fabricate the ZrO_2 layer at low temperature for triple-layer PSCs.

In order to assemble flexible triple-layer PSCs, a low-

Received date: 2022-03-21; **Revised date:** 2022-07-21; **Published online:** 2022-08-04
Foundation item: National Natural Science Foundation of China (52162020); Jiangxi Provincial Natural Science Foundation (20202BABL203012); Jiangxi Province Key Laboratory of Synthetic Chemistry (202005)
Biography: ZHANG Wanwen (1994–), male, Master candidate. E-mail: 2352937300@qq.com
张万文(1994–), 男, 硕士研究生. E-mail: 2352937300@qq.com
Corresponding author: LUO Jianqiang, professor. E-mail: luojianqiang@163.com; YANG Songwang, professor. E-mail: swyang@mail.sic.ac.cn
罗建强, 教授. E-mail: luojianqiang@163.com; 杨松旺, 研究员. E-mail: swyang@mail.sic.ac.cn

temperature method to fabricate ZrO_2 layer is necessary. In this work, a facile spray coating method was developed to fabricate porous ZrO_2 layer for TiO_2/ZrO_2/carbon triple-layer PSCs at low temperature using urea as porosity adjustor, which was well-compatible with flexible substrates, and easier to be scaled up than the conventional screen-printing method.

1 Experimental

1.1 Materials

Lead (II) iodide (PbI_2, 99%), methylammonium iodide (MAI, 99%), anhydrous *N*, *N*-dimethylformamide (DMF), titanium diisopropoxide bis(acetylace tonate) (75% in isopropanol), isopropanol, urea, $SrCl_2$ were purchased from Sigma-Aldrich. Zirconia was purchased from Aladdin. All chemicals were used as-received without further purification.

1.2 Perovskite solution

The perovskite solution was made by dissolving 0.159 g MAI, 0.461 g PbI_2 and 16 mg $SrCl_2$ in 1 mL DMF.

1.3 Zirconia ink for spray coating

0.5 g of ZrO_2 powder was dispersed in a mixed solution containing 5 mL H_2O and 5 mL isopropanol by sonification for 3 h. Urea was then added into the solution with $w(ZrO_2) : w(\text{urea})=2 : 1$.

1.4 Titania, zirconia and carbon pastes for screen-printing

Titania, zirconia and carbon pastes were prepared according to the previous report[27]. Typically, 1 g powder was dispersed in 20 mL ethanol under sonification. 0.5 g ethyl cellulose was dissolved in 4.5 g ethanol and 5 g terpineol. They were mixed together and then homogenized with ultra-sonification and ball milling for 10 h. Finally, ethanol was removed through rotary evaporation to form the paste.

1.5 Device fabrication

The solar cells were fabricated at room temperature under ambient air condition without using glove-box. Fluorine-doped tin dioxide (FTO) coated glass was patterned by 2 mol/L HCl solution and zinc powder, cleaned sequentially by detergent, deionized water and isopropanol, each for 30 min under ultrasonication. The compact titania (c-TiO_2) layer was prepared by spraying titanium diisopropoxide bis(acetylacetonate) in isopropanol (1 : 10 (in volume)) at 500 ℃ and annealed for 30 min. The mesoporous TiO_2 (m-TiO_2) layer was screen-printed on the c-TiO_2 layer and then annealed at 500 ℃ for 30 min. The zirconia ink was sprayed on the m-TiO_2 layer at 180 ℃ for 10–20 cycles, followed by washing in water. Afterwards, carbon paste was screen-printed on the ZrO_2 layer and sintered at 400 ℃ for 30 min. The titania and carbon layer were optimized to be 700 nm and 10 μm, respectively. Finally, PSCs were accomplished by drip-casting perovskite solution onto the carbon electrode and dried at 50 ℃ for 1 h (Fig. S1). For comparison, screen-printing method was used to fabricate the zirconia layer with the zirconia paste and sintered at 500 ℃ for 30 min. To build a PSC module, a 5-cell series was designed on a single FTO substrate as the previous report[27]. Zirconia layer was sprayed on the substrate covered with a metal patterned mask. The other fabrication process of the PSC module was the same to that of the single cell. The spray-coating was done with an Iwata HP-BP spray pen (3×10^5 Pa).

2 Results and discussion

Fig. 1(a) shows the structural schematic illustration of TiO_2/ZrO_2/carbon triple-layer PSCs, and the corresponding energy diagram is displayed in Fig. 1(b). The perovskite layer absorbs incident light to generate electrons and holes, which diffuse/transport to the interfaces. Then electrons are injected into the titania layer, and holes are transferred to the carbon electrode, respectively. According to the structure and mechanism of TiO_2/ZrO_2/carbon triple-layer PSCs, the porous zirconia layer takes important roles, not only separating the titania layer from the carbon electrode to avoid cell short circuit, but also providing a channel for perovskite to conduct electrons and holes.

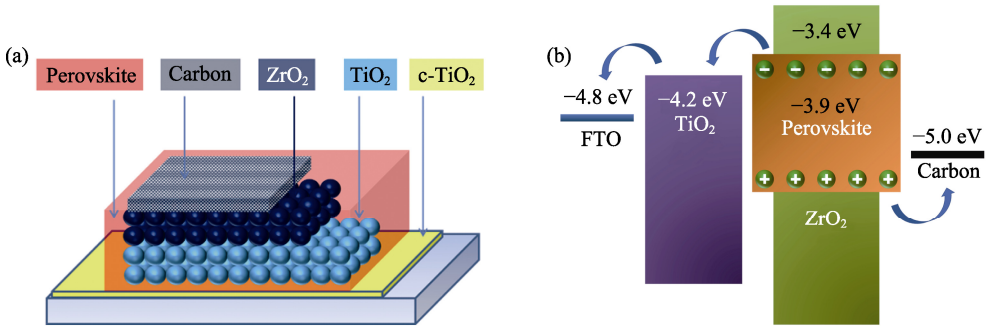

Fig. 1 Structural schematic illustration (a) and energy diagram (b) of TiO_2/ZrO_2/carbon triple-layer PSCs

However, the importance of fabrication of titania and carbon layers at low temperature were overestimated, while the zirconia layer was neglected by researchers. In order to assemble flexible triple-layer PSCs, high-quality zirconia layer prepared at low temperature is essential as well. Here, a low-temperature spray-coating method was developed to fabricate porous zirconia layer for high-performance TiO_2/ZrO_2/carbon triple-layer PSCs. Fig. S2(a) is the TEM image of zirconia particles. The size of the zirconia particles is 20–60 nm. XRD pattern (Fig. S2(b)) shows that the zirconia particles are well crystallized to afford monoclinic phase (JCPDS 65-1024). Before spraying, the zirconia particles were dispersed in the water and isopropanol solution to form a stable colloid, and urea was added. Fig. 2 shows SEM images of the zirconia films prepared by the spray-coating method. Without urea, the resultant zirconia film nearly doesn't contain any pore among zirconia particles (Fig. 2(a)). After the addition of urea, the pores in the zirconia film enlarged significantly. Fig. 2(b, c) compare SEM images of the zirconia films prepared with different ratios of zirconia to urea. It is observed that higher urea content results in larger pore size. Ammonia gases produced from decomposition of urea during spray process contribute to the formation of pores. These large pores in the zirconia film benefit the filling of perovskite into the underneath titania layer during the fabrication of TiO_2/ZrO_2/carbon triple-layer PSCs.

Fig. 3 compares the performance of the triple-layer PSCs with the zirconia layer prepared by the spray-coating method at different weight ratios of zirconia to urea. Without urea, the cell shows neglectable PCE, mainly attributed to the too small pores to fill the perovskite. After adding urea, their photovoltaic performance was dramatically promoted. PCE of PSCs with the zirconia layer prepared at *w*(zirconia) : *w*(urea)=2 : 1 and 1 : 1 reaches 8.43% and 11.6%, respectively. The formula of *w*(zirconia) : *w*(urea)=1 : 1 provided higher short-circuit current density (J_{sc}), resulting from better filling of the perovskite in the zirconia pores (Fig. 2(d, e)). In addition to control the porosity, there may be some N-containing species on the surface of zirconia, which lead to enhanced PCE[28-30]. To further confirm the effectiveness of spray-coating zirconia, hysteresis behaviors of PSC containing the zirconia layer prepared with *w*(zirconia) : *w*(urea)=1 : 1 were examined (Fig. 3(b)). PCE with forward scanning is 10.8%, up to 93.1% of PCE with reverse scanning, which shows good hysteresis performance.

Besides the porosity, the thickness of zirconia layer also greatly influences the performance of triple-layer PSCs. By fixing *w*(zirconia) : *w*(urea)=1 : 1, PSCs with different thicknesses of zirconia layer were fabricated by changing the spray-coating cycles. Fig. S3 shows the cross-sectional SEM images of the triple-layer PSCs with different thicknesses of zirconia layer before and after perovskite filling. 10, 15 and 20 cycles of spray coating produced zirconia films with the thicknesses of about 750, 1100 and 1500 nm, respectively. The titania and

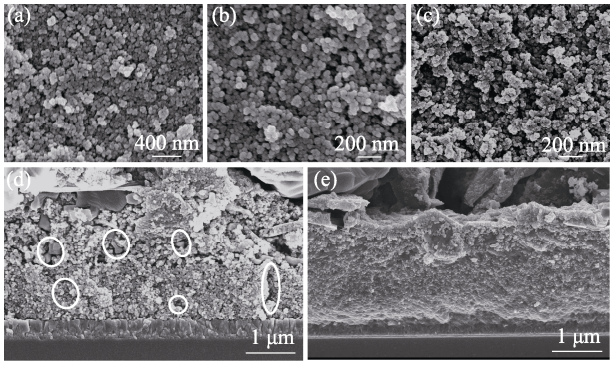

Fig. 2　SEM images of the zirconia film prepared by spray-coating without urea (a), with *w*(zirconia) : *w*(urea)= 2 : 1 (b) and 1 : 1 (c), cross-sectional SEM images of PSCs containing zirconia layer prepared with *w*(zirconia) : *w*(urea)= 2 : 1(d) and 1 : 1 (e)
Circled areas in (d) are not completely filled

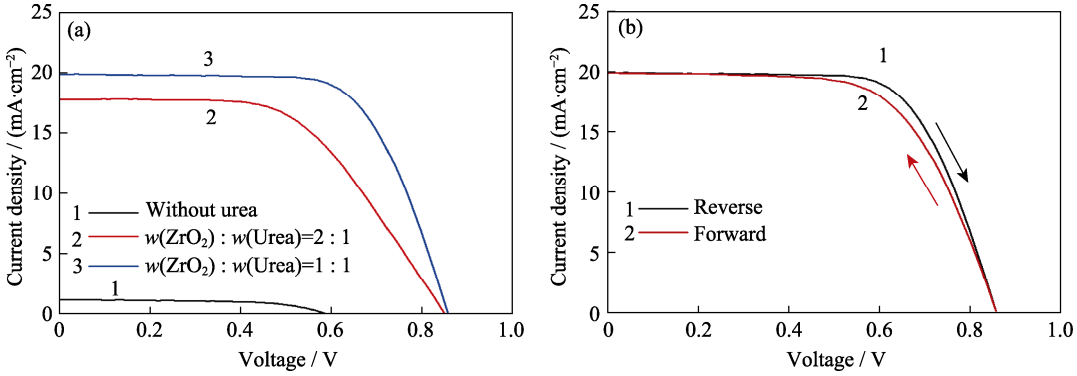

Fig. 3　*J-V* curves of PSCs prepared with *w*(zirconia) : *w*(urea)=2 : 1 and 1 : 1(a), and *J-V* curves from forward and reverse scanning of PSC prepared with *w*(zirconia) : *w*(urea)=1 : 1 (Zirconia layer thickness at ~1000 nm) (b)

carbon layer were optimized to be 700 nm and 10 μm, respectively, as previous report[16,27]. Perovskite could fully fill into all three porous zirconia films. Fig. 4(a) compares the corresponding *J-V* curves of three cells. Among them PSC with zirconia film thickness of 1100 nm displayed the highest PCE value (14.7%) with J_{sc} of 22.2 mA·cm^{-2}, open-circuit voltage (V_{oc}) of 0.93 V, and fill factor (FF) of 71.20%. Fig. 4(b) shows IPCE spectrum of the optimized chip, which display broad plateau in the wavelength from 380 to 750 nm with the highest value reaching 90%. The integrated current density from the incident-photon-to-current conversion efficiency (IPCE) spectrum reaches 20.94 mA·cm^{-2}, reasonably a little bit lower than J_{sc}. To demonstrate the reproducibility of fabrication and photovoltaic performance, a batch of 30 chips were fabricated with three different thicknesses of zirconia layer (10 chips per thickness). Fig. 4(c) summarizes their performances, the 1100 nm thick zirconia layer delivered a mean PCE of 13.9%, and a small standard deviation of 0.4454, suggesting excellent reproducibility of the spray-coating fabrication method. The PSCs output performance was tested at the fixed applied potential of 0.75 V. As shown in Fig. 4(d), PSC produces stable photocurrent density (19.1 mA·cm^{-2}) with corresponding PCE of 14.3%.

To demonstrate the effectiveness of this spray-coating method, its performance was compared with the conventional screen-printing method. PSCs with screen-printed zirconia layer were optimized to afford J_{sc}=22.23 mA·cm^{-2}, V_{oc}=0.960 V, FF=71.22% and PCE=15.2% (Fig. 4(a)). PCE of PSCs with spray-coated zirconia layer is slightly lower, mainly caused by the difference of V_{oc}. But the spray coating method spares the delicate process to prepare zirconia paste and high temperature to remove organic additives.

Benefitted from the low temperature process, the spray coating method could be used to prepare zirconia layer on flexible Polyethylene terephthalate (PET) substrate. The film with the thickness of 1.1 μm can tolerate high bending angle, as depicted in Fig. 5(a), mainly because the zirconia particles are not closely packed. Fig. 5(b) displays the photograph of the zirconia film on the flexible PET substrate bended to form a circle (ϕ4 cm). After 50 times bending cycles, the zirconia film keeps intact without cracks.

Film uniformity is critical for solar cell modules. Any defects in the film cause serious performance loss to the PSCs[7,31-32]. To verify the potential of our developed spray-coating method for large-area PSCs, rectangular triple-layer PSCs cells with active area of 2.5 cm×0.9 cm, and PSCs modules with 5 cells connected in series were fabricated (insets in Fig. S4(a, b)). To understand the effect of active area on cell performance, *J-V* curves were recorded with different illumination areas, which

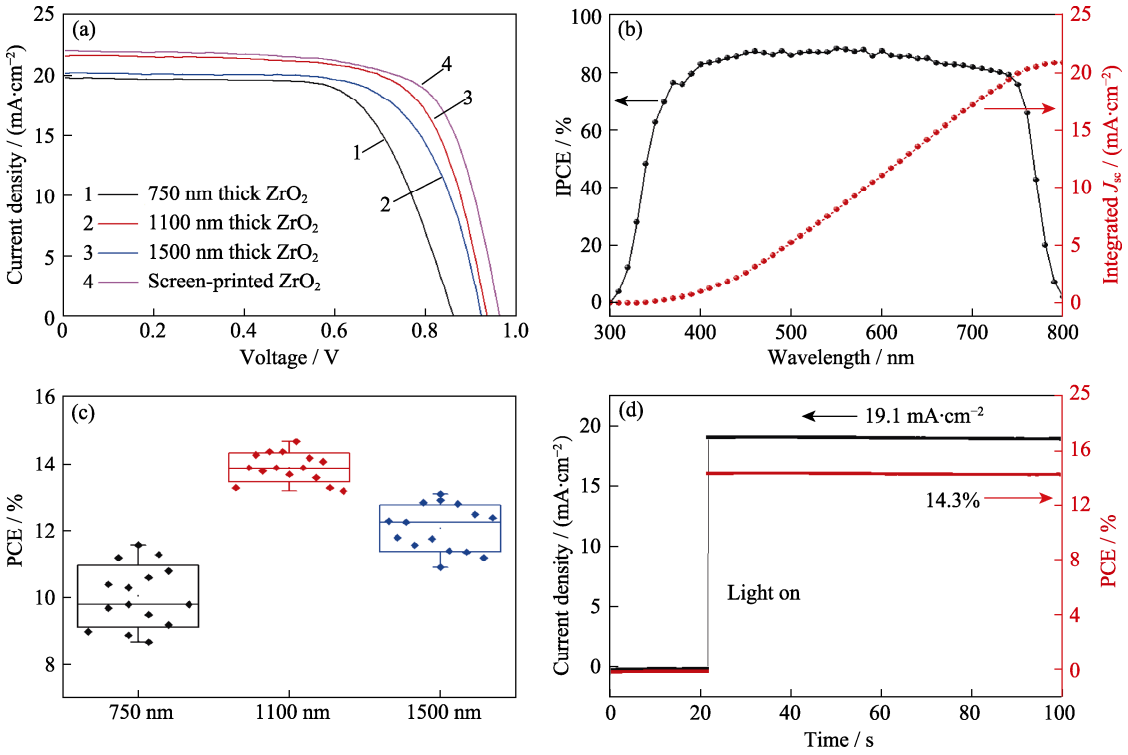

Fig. 4 *J-V* curves of the triple-layer PSCs with spray-coated and screen-printed zirconia layer(a), IPCE spectrum and corresponding integrated current density of the PSC with 1100 nm thick zirconia layer(b), PCE distribution of 30 chips with three different thicknesses of zirconia layer(c), and stabilized power output of PSCs with optimized spray-coated zirconia layer (d)

was precisely defined by a non-reflective aperture. PSCs with 0.126 cm^2 (ϕ4 mm aperture) and 0.196 cm^2 (ϕ5 mm aperture) illumination area displayed the same PCE (13.94%). PCE kept as high as 13.18% with larger illumination area (1.5 cm×0.8 cm), indicating high uniformity of the film. The decline of PCE for the cell with larger active area is mainly due to the decrease in FF, resulted from the increment of series resistance from FTO and carbon electrode. V_{oc} increases when the mask area approaches the cell size[33]. For practical application, large PSCs module with 5 cells connected in series on a single FTO substrate was fabricated (inset in Fig. S3(b)). *J*-*V* test shows that the PSCs module can deliver PCE= 10.8%, V_{oc}=4.49 V, J_{sc}=3.82 mA·cm^{-2} and FF=62.91%.

Stability poses a serious challenge for PSCs. The stability of the triple-layer PSCs with screen-printed and spray-coated zirconia layer was studied and compared. The initial PCE of the sprayed-coating zirconia PSC and screen-coating zirconia PSC is 13.2% and 14.1% respectively. As displayed in Fig. 6, both PSCs maintained excellent stability for 200 d without degradation when stored in a cabinet with constant temperature of 25 ℃ and relative humidity of 40%.

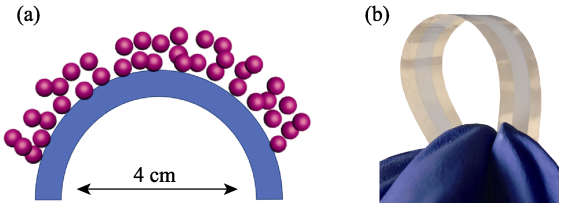

Fig. 5　Schematic illustration (a) and photograph (b) of the bending zirconia film on PET

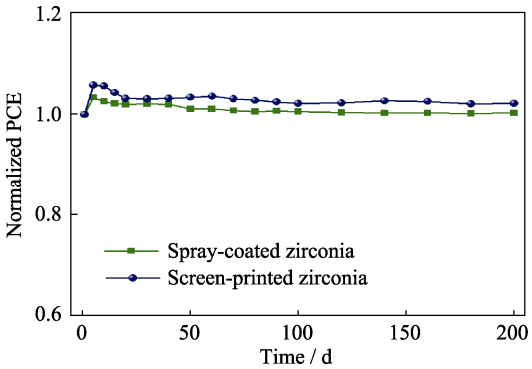

Fig. 6　Stability performance of PSCs with screen-printed and spray-coated zirconia layer

3　Conclusion

A facile low-temperature spray-coating method was developed to fabricate zirconia spacer for the TiO_2/ZrO_2/carbon triple-layer PSCs. The thickness and porosity of the zirconia spacer layer can be easily controlled by spray cycles and the urea content. The optimized PCE achieves 14.7% for the single cell and 10.8% for the module. Compared to conventional screen-printing method, the spray coating method developed in this work shows advantages of low-temperature process, less chemical usage, facile scale-up and compatibility with flexible substrate.

Supporting Materials

Supporting materials related to this article can be found at https://doi.org/10.15541/jim20220155.

References:

[1] KOJIMA A, TESHIMA K, SHIRAI Y, *et al.* Organometal halide perovskites as visible-light sensitizers for photovoltaic cells. *J. Am. Chem. Soc.*, 2009, **131(17):** 6050.

[2] LEE M M, TEUSCHER J, MIYASAKA T, *et al.* Efficient hybrid solar cells based on meso-superstructured organometal halide perovskites. *Science*, 2012, **338(6107):** 643.

[3] BURSCHKA J, PELLET N, MOON S J, *et al.* Sequential deposition as a route to high-performance perovskite-sensitized solar cells. *Nature*, 2013, **499(7458):** 316.

[4] HUANG L, ZHOU X, XUE R, *et al.* Low-temperature growing anatase TiO_2/SnO_2 multi-dimensional heterojunctions at MXene conductive network for high-efficient perovskite solar cells. *Nanomicro Lett.*, 2020, **12(1):** 44.

[5] PATIL P, MANN D S, NAKATE U T, *et al.* Hybrid interfacial ETL engineering using PCBM-SnS_2 for high-performance p-i-n structured planar perovskite solar cells. *Chem. Eng. J.*, 2020, **397:** 125504.

[6] JUNG E H, JEON N J, PARK E Y, *et al.* Efficient, stable and scalable perovskite solar cells using poly(3-hexylthiophene). *Nature*, 2019, **567(7749):** 511.

[7] PARK M, CHO W, LEE G, *et al.* Highly reproducible large-area perovskite solar cell fabrication via continuous megasonic spray coating of $CH_3NH_3PbI_3$. *Small*, 2019, **15(1):** 1804005.

[8] MCMEEKIN D P, MAHESH S, NOEL N K, *et al.* Solution-processed all-perovskite multi-junction solar cells. *Joule*, 2019, **3(2):** 387.

[9] YOO J J, SEO G, CHUA M R, *et al.* Efficient perovskite solar cells *via* improved carrier management. *Nature*, 2021, **590(7847):** 587.

[10] MEI A, LI X, LIU L, *et al.* A hole-conductor-free, fully printable mesoscopic perovskite solar cell with high stability. *Science*, 2014, **345(6194):** 295.

[11] TAN H, JAIN A, VOZNYY O, *et al.* Efficient and stable solution-processed planar perovskite solar cells *via* contact passivation. *Science*, 2017, **355(6326):** 722.

[12] LIU X, CHENG Y, LIU C, *et al.* 20.7% highly reproducible inverted planar perovskite solar cells with enhanced fill factor and eliminated hysteresis. *Energy Environ. Sci.*, 2019, **12(5):** 1622.

[13] ZHOU Z, LIAN H J, XIE J, *et al.* Non-selective adsorption of organic cations enables conformal surface capping of perovskite grains for stabilized photovoltaic operation. *Cell Reports Physical Science*, 2022, **3(2):** 100760.

[14] LIU X, LIAN H, ZHOU Z, *et al.* Stoichiometric dissolution of defective $CsPbI_2Br$ surfaces for inorganic solar cells with 17.5% efficiency. *Adv. Energy. Mater.*, 2022, **12(14):** 2103933.

[15] RONG Y, HU Y, MEI A, *et al.* Challenges for commercializing perovskite solar cells. *Science*, 2018, **361(6408):** eaat8235.

[16] LUO J, YANG H B, ZHUANG M, *et al.* Making fully printed perovskite solar cells stable outdoor with inorganic superhydrophobic coating. *J. Energy Chem.*, 2020, **50:** 332.
[17] YANG K, LIU S, DU J K, *et al.* Improving hole-conductor-free fully printable mesoscopic perovskite solar cells' performance with enhanced open-circuit voltage *via* the octyltrimethylammonium chloride additive. *Solar RRL*, 2021, **5(4):** 2000825.
[18] WANG Y, ZHANG T, XU F, *et al.* A facile low temperature fabrication of high performance $CsPbI_2Br$ all-inorganic perovskite solar cells. *Solar RRL*, 2018, **2(1):** 1700180.
[19] HU L, ZHAO Q, HUANG S, *et al.* Flexible and efficient perovskite quantum dot solar cells *via* hybrid interfacial architecture. *Nat. Commun.*, 2021, **12(1):** 466.
[20] YANG D, YANG R, ZHANG J, *et al.* High efficiency flexible perovskite solar cells using superior low temperature TiO_2. *Energy Environ. Sci.*, 2015, **8(11):** 3208.
[21] DAGAR J, CASTRO-HERMOSA S, GASBARRI M, *et al.* Efficient fully laser-patterned flexible perovskite modules and solar cells based on low-temperature solution-processed SnO_2/mesoporous-TiO_2 electron transport layers. *Nano Research*, 2018, **11(5):** 2669.
[22] YANG D, YANG R, PRIYA S, *et al.* Recent advances in flexible perovskite solar cells: fabrication and applications. *Angew. Chem. Int. Ed.*, 2019, **58(14):** 4466.
[23] MATSUI T, SEO J Y, SALIBA M, *et al.* Room-temperature formation of highly crystalline multication perovskites for efficient, low-cost solar cells. *Adv. Mater.*, 2017, **29(15):** 1606258.
[24] DI GIACOMO F, FAKHARUDDIN A, JOSE R, *et al.* Progress, challenges and perspectives in flexible perovskite solar cells. *Energy Environ. Sci.*, 2016, **9(10):** 3007.
[25] HAQUE S A, PALOMARES E, UPADHYAYA H M, *et al.* Flexible dye sensitised nanocrystalline semiconductor solar cells. *Chem. Commun.*, 2003, **(24):** 3008.
[26] JIANG P, JONES T W, DUFFY N W, *et al.* Fully printable perovskite solar cells with highly-conductive, low-temperature, perovskite-compatible carbon electrode. *Carbon*, 2018, **129:** 830.
[27] LUO J, CHEN J, WU B, *et al.* Surface rutilization of anatase TiO_2 for efficient electron extraction and stable P_{max} output of perovskite solar cells. *Chem*, 2018, **4(4):** 911.
[28] RONG Y, HOU X, HU Y, *et al.* Synergy of ammonium chloride and moisture on perovskite crystallization for efficient printable mesoscopic solar cells. *Nat. Commun.*, 2017, **8:** 14555.
[29] ZHANG Y H, LI Y. Interface materials for perovskite solar cells. *Rare Met.*, 2021, **40(11):** 2993.
[30] CHANG J H, LIU K, LIN S Y, *et al.* Solution-processed perovskite solar cells. *Journal of Central South University*, 2020, **27(4):** 1104.
[31] DENG Y, PENG E, SHAO Y, *et al.* Scalable fabrication of efficient organolead trihalide perovskite solar cells with doctor-bladed active layers. *Energy Environ Sci*, 2015, **8(5):** 1544.
[32] WU Y, YANG X, CHEN W, *et al.* Perovskite solar cells with 18.21% efficiency and area over 1 cm^2 fabricated by heterojunction engineering. *Nat Energy*, 2016, **1(11):** 16148.
[33] KIERMASCH D, GIL-ESCRIG L, BOLINK H J, *et al.* effects of masking on open-circuit voltage and fill factor in solar cells. *Joule*, 2019, **3(1):** 16.

氧化锆间隔层的低温喷涂制备及其三层结构钙钛矿太阳能电池应用性能

张万文[1], 罗建强[1], 刘淑娟[1], 马建国[1], 张小平[1], 杨松旺[2]

(1. 东华理工大学 江西省合成化学重点实验室, 南昌 330013; 2. 中国科学院 上海硅酸盐研究所, 中国科学院能量转换材料重点实验室, 上海 201899)

摘 要: 氧化钛/氧化锆/碳三层结构钙钛矿太阳能电池(Perovskite solar cells, PSCs)具有原材料廉价、制备工艺易放大和稳定性好等优势, 受到了广泛关注。但三层结构 PSCs 的低温制备研究进展缓慢, 主要原因之一在于难以在低温条件下构建合适的氧化锆间隔层。本研究以尿素为孔隙率调节剂, 用简单的喷涂法制备多孔氧化锆间隔层用于三层结构 PSCs。通过调节喷涂次数优化氧化锆层厚度为 1100 nm 时, 电池的性能最优, 单电池功率转换效率达到 14.7%, 5 块电池串联模块(5×0.9 cm×2.5 cm)达到 10.8%。PSCs 在恒温恒湿箱(25 ℃, 湿度 40%)保存 200 d, 功率转换效率保持稳定, 没有明显下降。柔性基底上的氧化锆层经 50 次弯曲测试后保持完整, 未见脱落。与传统的丝网印刷氧化锆间隔层制备方法相比, 本研究的喷涂方法具有方法简便、操作温度低、与柔性基底兼容性好的优点。

关 键 词: 钙钛矿太阳能电池; 三层结构; 低温; 氧化锆; 喷涂

中图分类号: TQ174 **文献标志码:** A

Supporting Materials:

Zirconia Spacer: Preparation by Low Temperature Spray-coating and Application in Triple-layer Perovskite Solar Cells

ZHANG Wanwen[1], LUO Jianqiang[1], LIU Shujuan[1], MA Jianguo[1], ZHANG Xiaoping[1], YANG Songwang[2]

(1. Jiangxi Province Key Laboratory of Synthetic Chemistry, East China University of Technology, Nanchang 330013, China; 2. CAS Key Laboratory of Materials for Energy Conversion, Shanghai Institute of Ceramics, Chinese Academy of Sciences, Shanghai 201899, China.)

Characterization

Without specific stated, the cells used in test were small sized cells with active area of 0.6 cm×0.8 cm. A picture of 30 cells is shown in Fig. S1. An aperture with 3 mm diameter is used to define the illustration area. Light illumination was performed using an Abet 2000 solar simulator. *J-V* curves were recorded on a Keithley 2400 source meter. The IPCE spectra were measured using a lock-in amplifier (Stanford Research Systems, SRS 810) with white light channeled from a Newport 300 W Xenon lamp through a 17 Hz mechanical chopper wheel and a monochromator (Oriel Cornerstone 130). For stability tests, PSCs were kept in an electronic cabinet with humidity of ~45%. X-ray diffraction (XRD) patterns were recorded on a Bruker D8 X-ray powder diffractometer. Transmission electron microscopy (TEM) images were taken on a JEOL JEM-2100 field emission electron microscope operated at 200 kV. Field emission scanning electron microscopy (FESEM) images were taken on a JEOL JSM-6701F electron microscope.

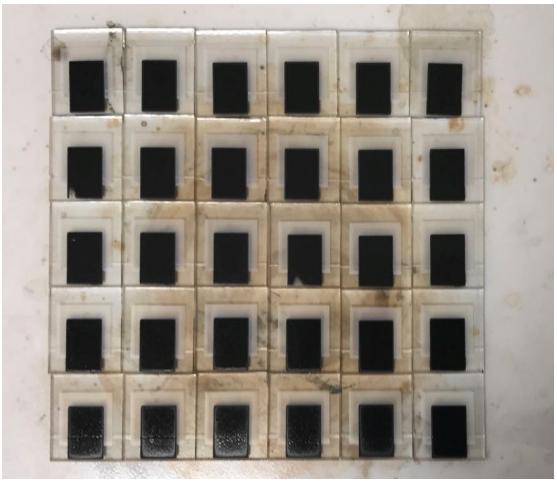

Fig. S1　Picture of 30 cells on a hotplate with active area of 0.6 cm×0.8 cm

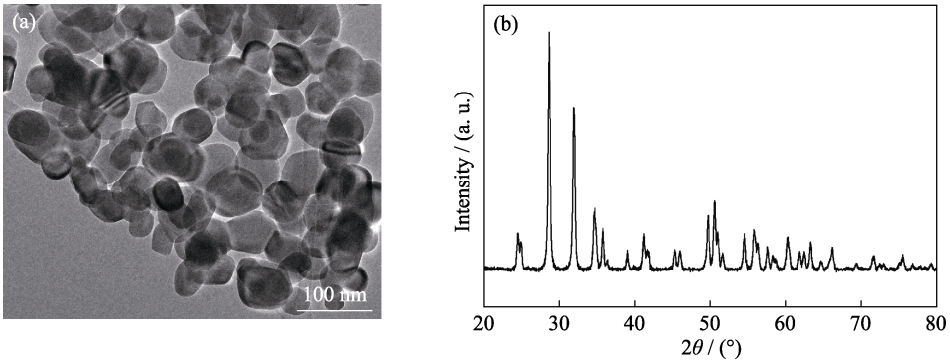

Fig. S2　(a) TEM image and (b) XRD pattern of the zirconia nanoparticles

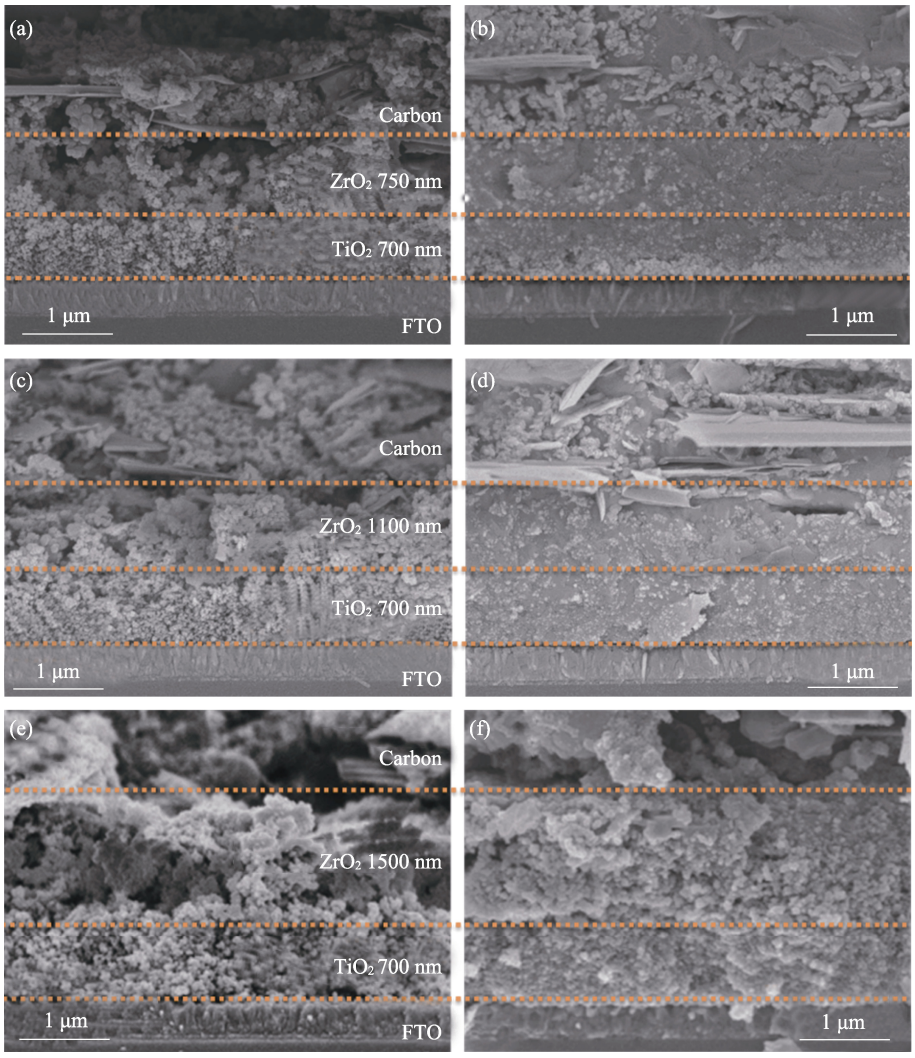

Fig. S3 Cross-sectional SEM images of PSCs before filling perovskite with the zirconia thickness of (a, b) 750, (c, d) 1100 nm and (e, f) 1500 nm（(a, c, e) before and (b, d, f) after filling perovkite）

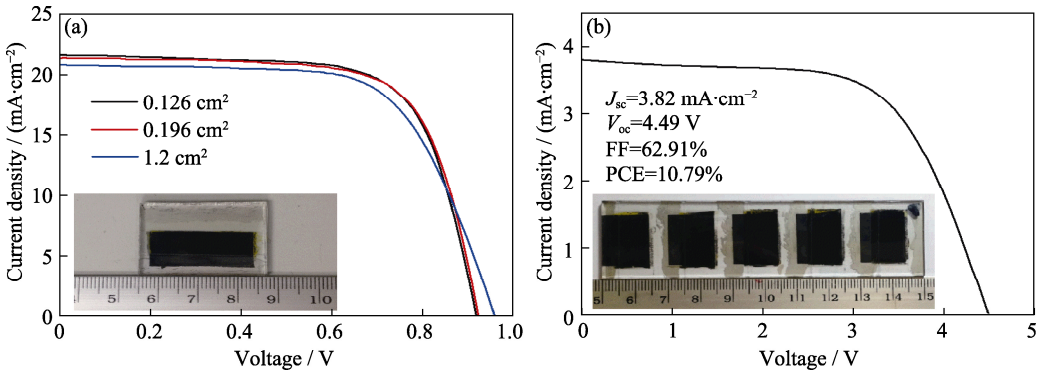

Fig. S4 (a) *J-V* curves of the cell with different illumination areas with inset showing the tested cell photograph; (b) *J-V* curve of PSCs module with five cells connected in series with inset showing the tested cell photograph